JOURNAL OF MATERIALS SCIENCE 14 (1979)1952–1960

Growth, morphology and slip system of α-Si_3N_4 single crystal

KOICHI NIIHARA, TOSHIO HIRAI
The Research Institute for Iron, Steel and Other metals, Tohoku University, Sendai 980, Japan

Under the conditions of growth temperatures 1500 to 1700° C and total gas pressure 10 to 50 Torr, α-Si_3N_4 single crystals have been grown by chemical vapour deposition from a mixture of NH_3, $SiCl_4$ and H_2. The crystals were transparent and brownish-red to colourless. The effects of the growth conditions on the crystal morphology, growth habit and growth direction have been investigated. On the basal and prismatic planes, the variation in Knoop hardness with orientation of the indenter long-axis has been measured at temperatures up to 1500° C; maximum hardness values were obtained along the $\langle 1\,0\,\bar{1}\,0\rangle$ direction for the basal plane and along the [0 0 0 1] directions for the prismatic planes. Hardness anisotropy analysis suggests that the active slip systems of α-Si_3N_4 are $\{1\,0\,\bar{1}\,0\}$ [0 0 0 1] from room temperature to 1500° C.

1. Introduction

There is considerable interest in the use of ceramics as components of high-temperature gas turbines in order to increase the efficiency. Silicon nitride (Si_3N_4) is a most promising material as a part or an assembly of gas turbines operating under high stresses [1]. Therefore, studies on the high-temperature mechanical properties of Si_3N_4 are essential.

In general, Si_3N_4 is available in three different forms as the bulk material; reaction-sintered, hot-pressed and chemical vapour-deposited Si_3N_4 [1–5]. Mechanical properties of these Si_3N_4 are affected by impurities, additives, voids and microstructures. In order to know the intrinsic mechanical properties of Si_3N_4, especially for the slip system, further studies on its single crystal are needed.

The single crystals of Si_3N_4 have been prepared by various methods [6–15]. The crystals are obtained in the form of whiskers, needles or platelets and are mainly used for crystallographic studies. They are too small to investigate the mechanical properties of an Si_3N_4 single crystal, and there are many points to be elucidated as to the slip system of α-Si_3N_4.

Brookes *et al.* [16] have shown that the active slip systems can be determined by the anisotropy in hardness for different crystallographic planes. The validity of their model has been demonstrated for various elements and compounds [16–23]. The main objectives of the present work are to prepare α-Si_3N_4 single crystals of sufficiently large size to investigate the hardness anisotropy and to determine the slip system at high temperatures. The effects of the growth conditions on the crystal growth and morphology of α-Si_3N_4 single crystals are also discussed.

2. Results and discussion

2.1. Crystal growth

Si_3N_4 single crystals have been grown by various methods such as chemical vapour deposition (CVD) from $SiH_4 + NH_3 + H_2$ and $SiCl_4 + N_2 + H_2$ systems [6, 11], nitriding of Si powder [10], heat-treatment of hot-pressed Si_3N_4 [9], growth from Si melts [7, 8] and sublimation of Si_3N_4 [14]. In this work, the Si_3N_4 single crystals were grown on a directly heated graphite substrate by CVD from a mixture of NH_3 and H_2-carried $SiCl_4$. The growth process and experimental set-up used in the present experiments are similar to those previously reported [4].

The crystal growth in the CVD method is well

 0022–2461/79/081952–09 $02.90/0

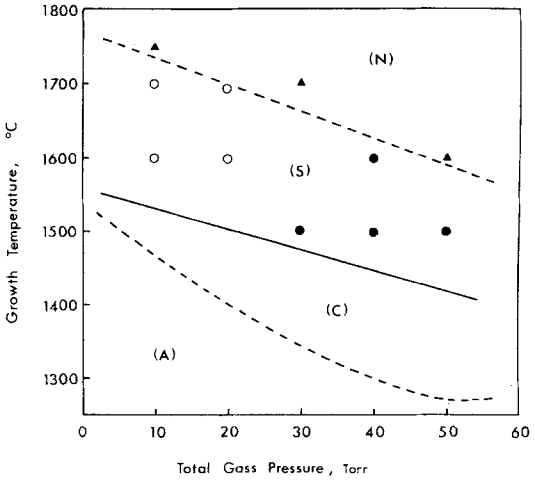

Figure 1 Effect of growth temperature and total gas pressure on the crystal growth of Si_3N_4. (A) plate-like amorphous Si_3N_4, (C) plate-like polycrystalline α-Si_3N_4, (S) α-Si_3N_4 single crystals with needle-like (○) and pyramidal (●) forms, (N) no deposits (▲).

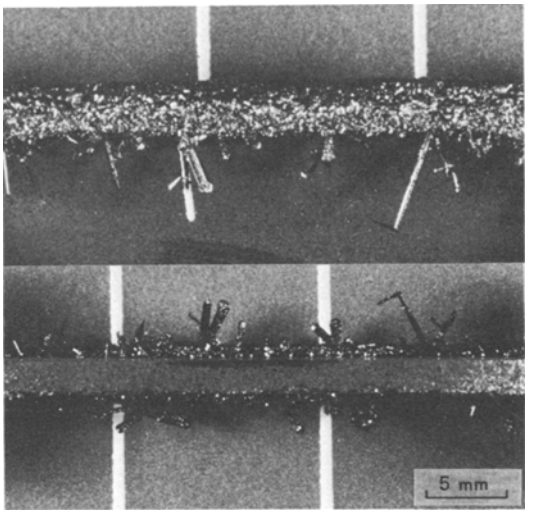

Figure 3 Needle-like α-Si_3N_4 single crystals grown under growth conditions of 1700° C and 10 Torr. 1 division = 12 mm.

known to depend strongly on the gas concentration, gas flow rate, growth temperature, total gas pressure, growth time, etc. In this work, the flow rates of NH_3, $SiCl_4$ and H_2 were fixed at 60, 170 and 700 $cm^3\ min^{-1}$, respectively, and the influences of the growth temperature and the total gas pressure on the crystal growth were examined.

As shown in Fig. 1, amorphous Si_3N_4 and polycrystalline α-Si_3N_4 in plate-like form were deposited in regions A and C, respectively, and no deposition occurred in region N [4]. On the other hand, the crystals grown in region S were confirmed to be single crystals of α-Si_3N_4 from X-ray precession and Laue techniques. These crystals were transparent and appeared to be coloured from brownish-red to colourless. Typical X-ray precession photographs obtained are shown in Fig. 2a and b, which were identified as diffraction patterns of α-Si_3N_4 single crystals whose surfaces are parallel to the (0 0 0 1) and $\{1\,0\,\bar{1}\,0\}$ planes, respectively. X-ray powder diffraction did not reveal the β-phase in the crystals.

2.2. Morphology

The relationships of the growth conditions to the structure, size and morphology of Si_3N_4 single crystals are listed in Table I. For α-Si_3N_4 single crystals, four types of morphology (whisker, needle, prism and platelet) have been observed,

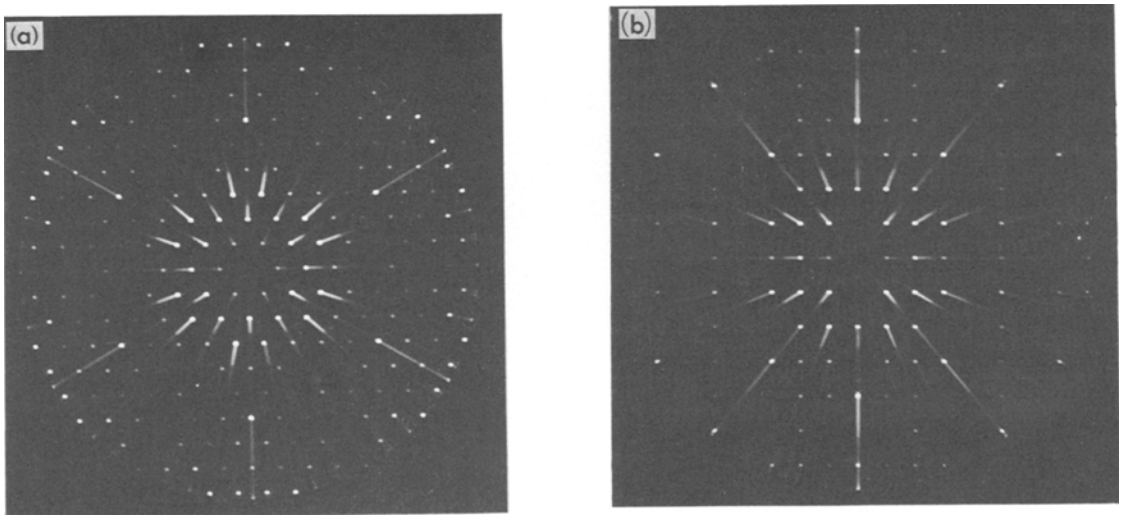

Figure 2 Typical precession photographs of α-Si_3N_4 single crystals (Zr-filtered Mo$K\alpha$ radiation). (a) (0 0 0 1), (b) $\{1\,0\,\bar{1}\,0\}$.

TABLE I Growth, morphology and size of Si_3N_4 single crystals grown by various methods

Method	Conditions		Structure*	Morphology	Size	Reference
	Temperature (° C)	Pressure (Torr)				
CVD of $SiH_4 + NH_3 + H_2$	1200	760	α	Needle	–	[11]
CVD of $SiCl_4 + N_2 + H_2$	1500 ~ 1700	760	α	Prism	0.1 ~ 0.5 mm in length	[6]
Nitriding of Si powder	1240 ~ 1420	760 (N_2)	α	Whisker or flattened needle	–	[10, 15]
Heating of hot-pressed Si_3N_4	1800	1422 (N_2)	α	Platelet	0.4 mm × 0.27 mm × 0.03 mm	[9]
Sublimation of Si_3N_4	1700	760 (N_2)	β	Whisker	0.1 ~ 0.5 mm in length	[14]
Growth from Si melts	1650	760 (N_2)	β	Needle	0.1 ~ 0.3 mm in diameter	[7, 8]
CVD of $SiCl_4 + NH_3 + H_2$	1600 ~ 1700	10 ~ 20	α	Needle	1.5 mm^2 × 15 mm	This work
CVD of $SiCl_4 + NH_3 + H_2$	1500 ~ 1600	30 ~ 50	α	Pyramid	2 ~ 3 mm across	This work

* α, α-Si_3N_4; β, β-Si_3N_4.

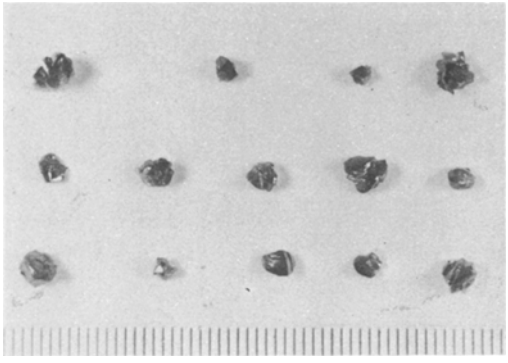

Figure 4 Pyramidal α-Si_3N_4 single crystals grown under conditions of 1500° C and 40 Torr. 1 division = $\frac{2}{3}$ mm.

probably due to the different growth conditions as can be seen from Table I.

The morphology of α-Si_3N_4 single crystals obtained in this work was needle-like and pyramidal. These depended markedly on the growth temperature and the total gass pressure as shown in Fig. 1. Needle-like α-Si_3N_4 single crystals were grown at growth temperatures of 1600 and 1700° C and total gas pressures of 10 and 20 Torr. The maximum size was 1.5 mm^2 cross-section and 15 mm long. Fig. 3 shows examples of the single crystals which were grown at 1700° C and 10 Torr. The pyramidal α-Si_3N_4 single crystals were obtained at growth temperatures of 1500 and 1600° C and total gas pressures of 30 to 50 Torr. The crystals obtained were 2 to 3 mm across as displayed in Fig. 4.

2.3. Growth direction and habit

Four growth directions of [0 0 0 1], $\langle 1\,1\,\bar{2}\,0\rangle$, $\langle 1\,0\,\bar{1}\,1\rangle$ and $\langle 1\,0\,\bar{1}\,3\rangle$ have been reported for the whisker-like α-Si_3N_4 [6, 12]. The needle-like Si_3N_4 obtained in this work was identified to be mainly grown along the [0 0 0 1] and $\langle 1\,1\,\bar{2}\,0\rangle$

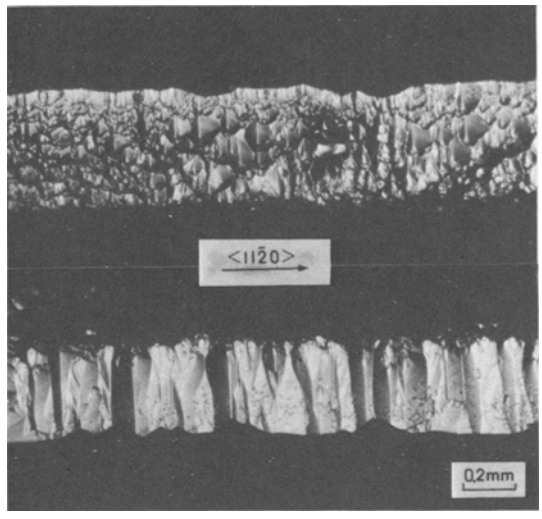

Figure 6 Growth habit of needle-like α-Si_3N_4 single crystals grown in the $\langle 1\,1\,\bar{2}\,0\rangle$ direction under growth conditions of 1700° C and 20 Torr.

directions. The variation in the growth direction with the growth conditions was observed: α-Si_3N_4 single crystals grew preferentially in the [0 0 0 1] direction at 1600° C and in the $\langle 1\,1\,\bar{2}\,0\rangle$ direction at 1700° C. The needles grown along the *c*-axis were hexagonal and their faces were found to be very smooth and flat without any characteristic surface structure as shown in Fig. 5. On the other hand, the needles grown in the $\langle 1\,1\,\bar{2}\,0\rangle$ direction were octahedral and these were formed by two sets of the (0 0 0 1), $\{1\,0\,\bar{1}\,0\}$, $\{1\,0\,\bar{1}\,2\}$ and $\{1\,0\,\bar{1}\,3\}$ planes. The growth habits were observed for the $\{1\,0\,\bar{1}\,2\}$ and $\{1\,0\,\bar{1}\,3\}$ planes as presented in Fig. 6 and not for the (0 0 0 1) and $\{1\,0\,\bar{1}\,0\}$ planes.

In some of the needles, the growth direction varied from $\langle 1\,1\,\bar{2}\,0\rangle$ to [0 0 0 1], probably due

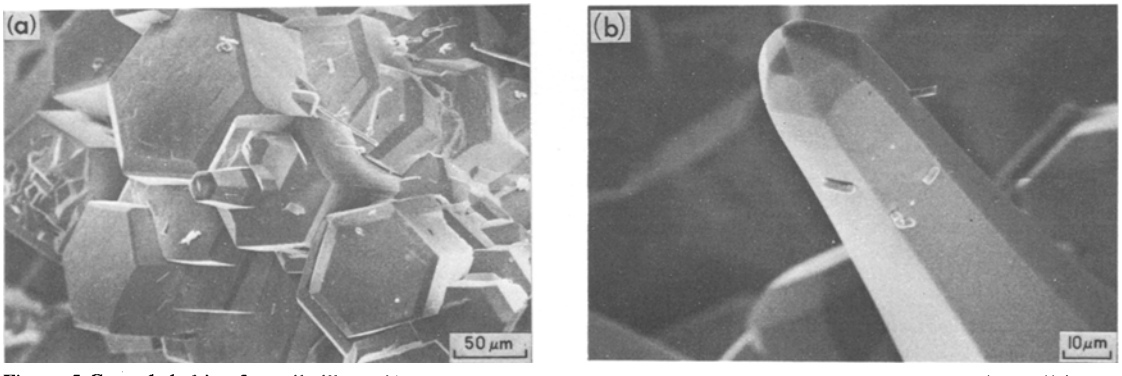

Figure 5 Growth habit of needle-like α-Si_3N_4 single crystals grown in the *c*-axis direction under growth conditions of 1600° C and 20 Torr (a). (b) Higher magnification of (a).

TABLE II Some properties of α-Si_3N_4 single crystals

Growth conditions	Colour	Density* ($g\,cm^{-3}$)		Lattice constants†			Oxygen content‡ (wt%)
		ρ_{th}	ρ_{ob}	a (Å)	c (Å)	Volume $(Å)^3$	
1700° C, 10 Torr	Colourless	3.179	3.18	7.759 (2)	5.628 (2)	293.4	< 0.1
1600° C, 20 Torr	Brown	3.181	3.17	7.754 (2)	5.625 (3)	292.9	~ 0.3
1500° C, 40 Torr	Brownish-red	3.182	3.17	7.753 (2)	5.625 (2)	292.8	~ 0.3

* ρ_{th} theoretical density, ρ_{ob} observed density.
† The standard deviation is shown as 7.759 (2) for 7.759 ± 0.002.
‡ Values estimated from a relationship between oxygen content and unit cell volume [24].

to the variation in the growth temperature as shown in Fig. 3.

2.4. Crystal characterization

The lattice constants and density of α-Si_3N_4 single crystals were measured by means of an X-ray powder camera and a displacement technique using toluene, respectively. The results are summarized in Table II. In this table, the colour and oxygen content estimated from the unit cell volume [24] are also shown.

Si_3N_4 is essentially transparent and colourless because of its optical absorption edge being about 3100 Å [25]. Indeed, α-Si_3N_4 single crystals containing a small amount of oxygen (0.003%) have been found to be transparent and colourless [26]. Moreover, the unit cell volume of α-Si_3N_4 increases with decreasing oxygen content [24, 25]. In the present work, similar behaviour was observed as shown in Table II.

2.5. Hardness anisotropy at room temperature

Relatively large α-Si_3N_4 single crystals obtained in the present work were cut into 0.5 mm thick slices parallel to the (0 0 0 1), $\{1\,0\,\bar{1}\,0\}$ and $\{1\,1\,\bar{2}\,0\}$ planes. Orientation analyses using an X-ray precession technique were then performed. After mechanically polishing to a 0.25 μm diamond finish, Knoop hardness measurements were made as a function of indenter long-axis orientation on each crystallographic plane under the condition of 100 g load, 0.3 mm sec^{-1} loading rate and 10 sec loading time [27].

Figs. 7 to 9 present the variation in hardness with orientation of the indenter long-axis on the basal (0 0 0 1), prismatic $\{1\,0\,\bar{1}\,0\}$ and prismatic $\{1\,1\,\bar{2}\,0\}$ planes of α-Si_3N_4 at room temperature, respectively. As shown in these figures, the hardness was strongly dependent on the crystallographic plane and the indenter orientation. On the prismatic planes, the hardness was largest when the long axis of the indenter was directed toward the c-axis and was smallest when directed toward the direction normal to the c-axis. The difference in hardness between the two directions was about 11%. The basal plane showed a small but significant amount of hardness anisotropy, about 5%, indicating a maximum along $\langle 1\,0\,\bar{1}\,0\rangle$ and a minimum along $\langle 1\,1\,\bar{2}\,0\rangle$. The present result

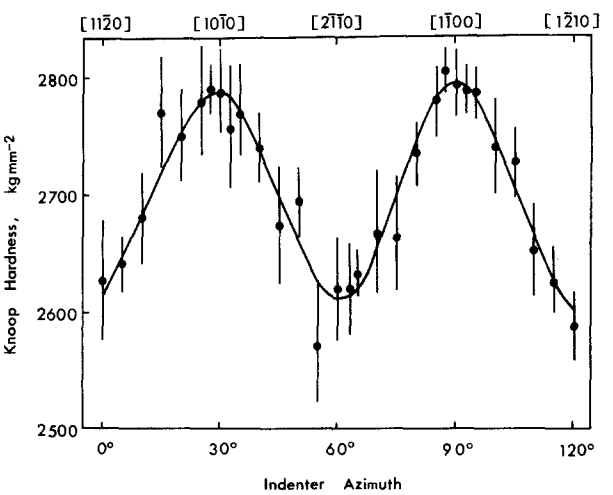

Figure 7 Variation in Knoop hardness with the indenter long-axis angle from $[1\,1\,\bar{2}\,0]$ for a (0 0 0 1) plane of α-Si_3N_4 (100 g load).

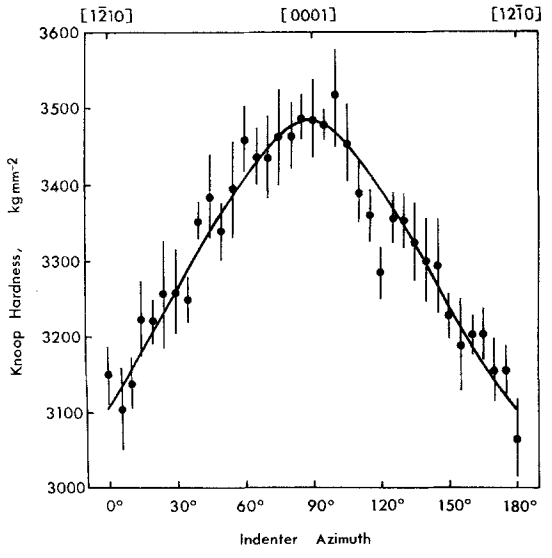

Figure 8 Variation in Knoop hardness with the indenter long-axis angle from [1 $\bar{2}$ 1 0] for $\{1\,0\,\bar{1}\,0\}$ planes of α-Si_3N_4 (100 g load).

that the hardness anisotropy was not so pronounced on the basal plane corresponds to those reported for a large number of hexagonal crystals such as Al_2O_3, TiB_2, HfB_2, Mo_2C and SiC [16, 22, 28]. This can be expected from the fact that the three *a*-axis form an equilateral triangle and have a theoretically equal bond strength [28]. A remarkable orientation-dependence of cracking has been reported for Al_2O_3 and SiC [16, 17, 29]. In this work, in almost all cases under a 100 g load the cracks were not observed as reported previously [30].

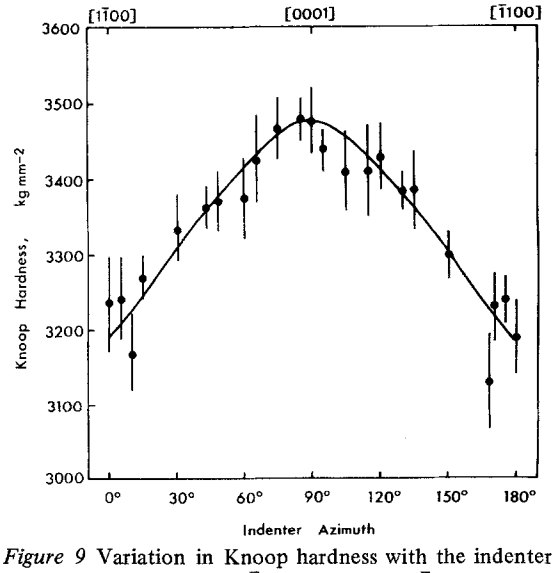

Figure 9 Variation in Knoop hardness with the indenter long-axis angle from [1 $\bar{1}$ 0 0] for a $\{1\,1\,\bar{2}\,0\}$ plane of α-Si_3N_4 (100 g load).

2.6. Temperature dependence of hardness anisotropy

With the long axis-orientation where the maximum and minimum hardness occurred at room temperature as shown in Figs. 7 to 9, the hot hardnesses were measured, under the same conditions as the room temperature tests, up to 1500° C in vacuum of $\sim 10^{-5}$ Torr or highly pure Ar atmosphere using a high-temperature hardness tester (NIKON, Model: QM) [21]. The damage caused to a diamond indenter tip by chemical reaction with the specimen occurred at temperatures above 1300° C for some polycrystalline CVD-Si_3N_4 [31] and not for α-Si_3N_4 single crystals. This may be attributed to the difference in the amount of impurities, most likely oxygen, as discussed in Section 2.4.

Plots of logarithmic hardness versus temperature are shown in Fig. 10. The hardness value at each temperature was obtained by taking the mean of at least ten indentations on two slices with the same orientation. The experimental error in the hot-hardness measurements was

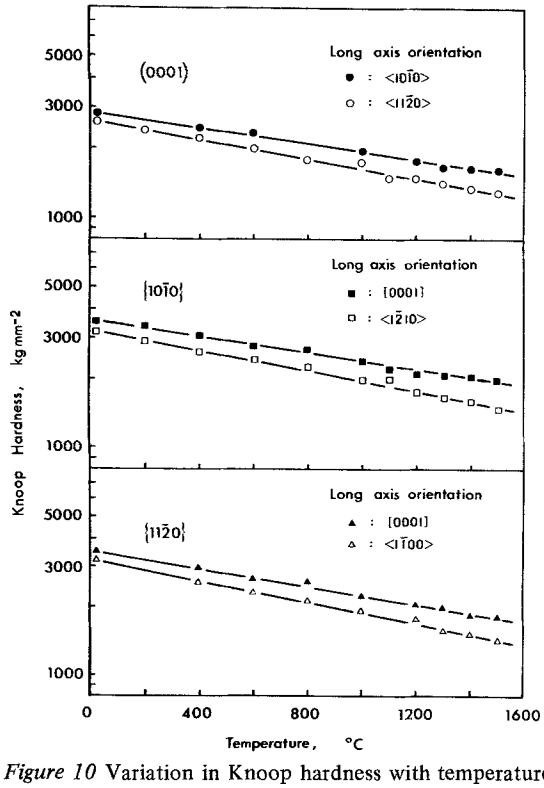

Figure 10 Variation in Knoop hardness with temperature for the basal and prismatic planes of α-Si_3N_4 single crystals (100 g load).

within 2.7% in the whole temperature range investigated. The hardness hysteresis and structure change (α to β transformation) were not observed during heating and cooling experiments.

As shown in Fig. 10, the logarithmic hardness decreased linearly with increasing temperature in all crystallographic planes. The inclination was slightly affected by the crystallographic plane and the indenter orientation, and the hardness anisotropy was emphasized at higher temperatures. This indicates that the deformation mechanism does not vary with temperature. Another striking feature of Fig. 10 is that α-Si_3N_4 has extremely high hardness above $1200\,kg\,mm^{-2}$ even at 1500° C. Such high-temperature hardness has not been reported for other refractory materials [22, 32–34].

The surfaces of Si_3N_4 single crystals were thermally etched slightly in a highly pure Ar atmosphere at temperatures above 1400° C. However, etch pits or slip lines which indicate indirectly the dislocation motion could not be detected around indentations.

The loading time dependence of hardness was also examined from 1 to 100 sec at 1400 and 1500° C for some specimens. The decrease in hardness value with loading time was much smaller than that of SiC reported in a separate paper [35], as expected from the high hot-hardness.

2.7. Slip system

Evans and Sharp [36] have found from the transmission electron microscopic observations of reaction-sintered and hot-pressed Si_3N_4 that β-Si_3N_4 grains contain dislocations having a [0 0 0 1] Burgers vector which is likely to be most mobile with $\{1\,0\,\bar{1}\,0\}$ as the primary slip plane. Kossowsky [37] reported that the most common Burgers vector of dislocations contained in α and β grains of hot-pressed Si_3N_4 is [0 0 0 1]. However, the dislocation motion in deformed Si_3N_4 was not observed.

Under the stress system involving the large hydrostatic component as in the case of hardness testing, the indenter inhibits brittle failure and makes the materials yield in a plastic manner. Brookes *et al.* [16] have shown that the hardness anisotropy in a single crystal can be interpreted by the magnitude of the "effective resolved shear stress" (τ_e') beneath the indenter acting on the primary slip system of a crystal. τ_e' is given by the following equation [16]:

$$\tau_e' = (F/A)\cos\lambda\cos\phi\,(1/2)(\cos\psi + \sin\nu),$$
$$\lambda = (F/A)f(\lambda, \phi, \psi, \nu), \tag{1}$$

where F is the applied force, A is the cross-sectional area, λ is the angle between the stress axis and the slip direction, ϕ is the angle between the stress axis and the normal to the slip plane, ψ is the angle between the indenter face and the axis of rotation in the slip plane, and ν is the angle between the slip direction and a horizontal axis parallel to the indenter face. Then, the factor f^{-1} $(\lambda, \phi, \psi, \nu)$ describes the hardness anisotropy. For various materials with different structures, it is reported that the active slip systems determined from Equation 1 by considering the data on the hardness anisotropy agree very well with those verified by other techniques such as the dislocation etch pit and slip line analyses [16–23, 27]. Therefore, in this work we have also attempted to reveal the active slip system of α-Si_3N_4 from the relation of the factor f^{-1} with the observed hardness anisotropy.

Table III shows the minimum f^{-1} values in various indentation directions and planes, which were calculated using Equation 1 for the common slip systems of $\{1\,0\,\bar{1}\,0\}\langle 1\,1\,\bar{2}\,0\rangle$, $(0\,0\,0\,1)\langle 1\,1\,\bar{2}\,0\rangle$ and $\{1\,0\,\bar{1}\,0\}$ [0 0 0 1] in hexagonal crystals [16, 22]. From this table, it is clear that the following relationships in hardness values will be obtained for each sytem under consideration.

For the $(0\,0\,0\,1)\langle 1\,1\,\bar{2}\,0\rangle$ slip system,

$$\begin{aligned} H_{(0001)[10\bar{1}0]} &< H_{(0001)[11\bar{2}0]} \\ H_{(10\bar{1}0)[0001]} &> H_{(10\bar{1}0)[1\bar{2}10]} \\ H_{(11\bar{2}0)[0001]} &> H_{(11\bar{2}0)[1\bar{1}00]} \end{aligned} \tag{2}$$

For the $\{1\,0\,\bar{1}\,0\}\langle 1\,1\,\bar{2}\,0\rangle$ slip system,

$$\begin{aligned} H_{(0001)[10\bar{1}0]} &> H_{(0001)[11\bar{2}0]} \\ H_{(10\bar{1}0)[0001]} &< H_{(10\bar{1}0)[1\bar{2}10]} \\ H_{(11\bar{2}0)[0001]} &< H_{(11\bar{2}0)[1\bar{1}00]} \end{aligned} \tag{3}$$

For the $\{1\,0\,\bar{1}\,0\}\langle 0\,0\,0\,1\rangle$ slip system,

$$\begin{aligned} H_{(0001)[10\bar{1}0]} &> H_{(0001)[11\bar{2}0]} \\ H_{(10\bar{1}0)[0001]} &> H_{(10\bar{1}0)[1\bar{2}10]} \\ H_{(11\bar{2}0)[0001]} &> H_{(11\bar{2}0)[1\bar{1}00]}. \end{aligned} \tag{4}$$

Here the first and second suffixes of the hardness (H) represent the indentation plane and the orientation of the long-axis of the Knoop indenter, respectively.

TABLE III Comparison between Knoop hardness of α-Si_3N_4 single crystal and f^{-1} values for typical slip systems of hexagonal crystals in various indentation planes and directions

Indentation plane	(0 0 0 1)		(1 0 $\bar{1}$ 0)		(1 1 $\bar{2}$ 0)	
Indenter long-axis orientation	[1 0 $\bar{1}$ 0]	[1 1 $\bar{2}$ 0]	[0 0 0 1]	[1 $\bar{2}$ 1 0]	[0 0 0 1]	[1 $\bar{1}$ 0 0]
Value of f^{-1}						
(0 0 0 1) ⟨1 1 $\bar{2}$ 0⟩ slip [16, 22]	2.7	3.0	17.4	3.0	15.1	2.7
{1 0 $\bar{1}$ 0} ⟨1 $\bar{2}$ 1 0⟩ slip [16, 22]	18.1	6.4	2.2	44.2	2.6	31.1
{1 0 $\bar{1}$ 0} [0 0 0 1] slip	3.1	2.6	46.6	2.6	37.5	2.9
Knoop hardness (kg mm^{-2})						
Room temperature	2791	2620	3486	3151	3476	3276
1500° C	1522	1263	1935	1476	1802	1432

The relationships in the observed hardness anisotropy for α-Si_3N_4 (see Figs. 7 to 10 and Table III) are in accord with the case of (4) through all the testing temperatures. This implies that the active slip system of α-Si_3N_4 is {1 0 $\bar{1}$ 0} [0 0 0 1] over the temperature range from room temperature to 1500° C, as in the case of β-Si_3N_4 [36].

3. Conclusions

(1) Relatively large single crystals of α-Si_3N_4 were successfully grown under the conditions of growth temperatures of 1500 to 1700° C and total gas pressures of 10 to 50 Torr by a CVD method. The maximum size was 1.5 mm^2 cross-section and 15 mm long for the needle-like crystals and 2 to 3 mm across for the pyramidal crystals. The crystals were transparent and brownish-red to colourless.

(2) The morphology of single crystals depended mainly on the total gas pressure. The needle-like crystals were obtained at 10 and 20 Torr, and the pyramidal crystals were obtained at 30 to 50 Torr. The growth direction of needle-like crystals was affected by the growth temperature: [0 0 0 1] at 1600° C and ⟨1 1 $\bar{2}$ 0⟩ at 1700° C.

(3) The colourless single crystals were larger in unit cell volume and smaller in oxygen content than the brownish-red ones.

(4) The Knoop hardness of α-Si_3N_4 single crystals was remarkably dependent on the crystallographic plane and the indenter long-axis orientation. The maximum and minimum hardnesses were observed along the ⟨1 0 $\bar{1}$ 0⟩ and ⟨1 1 $\bar{2}$ 0⟩ directions for the (0 0 0 1) plane, respectively, and along the directions parallel and normal to the c-axis for the {1 0 $\bar{1}$ 0} and {1 1 $\bar{2}$ 0} planes, respectively.

(5) The hot hardness was measured at temperatures up to 1500° C for various indentation directions and planes. The logarithmic hardness decreased linearly with increasing temperature, maintaining the same hardness anisotropy as that at room temperature.

(6) An analysis of hardness anisotropy by the "effective resolved shear stress" beneath the indenter revealed that the active slip system of α-Si_3N_4 is {1 0 $\bar{1}$ 0} [0 0 0 1] from room temperature to 1500° C.

Acknowledgement

This research was financially supported by the Ministry of Education, Contract nos. 285168 and 265212.

References

1. D. J. GODFREY, *Metal and Materials* **2** (1968) 305.
2. N. L. PARR and E. R. W. MAY, *Proc. Brit. Ceram. Soc.* 7 (1967) 81.
3. R. F. COE, R. J. LUMBY and M. F. PAWSON, "Special Ceramics 5", edited by P. Popper (British Ceramic Research Association, Stoke-on-Trent, 1972) p. 361.
4. K. NIIHARA and T. HIRAI, *J. Mater. Sci.* **11** (1976) 593.
5. R. J. TANZILLI, J. J. GEBHARDT and J. O. HANSON, G. E. Report, Doc. No. 77SDR2257, Contract No. N00014-76-C-0547 (1977).
6. K. KIJIMA, N. SETAKA and H. TANAKA, *J. Crystal Growth* **24/25** (1974) 183.
7. K. INOMATA and T. YAMANE, *ibid* **21** (1974) 317.
8. W. KAISER and C. D. THURMOND, *J. Appl. Phys.* **30** (1959) 427.
9. I. KOHATU and J. M. MACCAULEY, *Mater. Res. Bull.* **9** (1974) 917.
10. P. POPPER and S. N. RUDDLESDEN, *Trans. Brit. Ceram. Soc.* **60** (1951) 603.
11. K. E. BEAN, P. S. GLEIM, R. L. YEAKLEY and W. R. RUNYAN, *J. Electrochem. Soc.* **114** (1967) 733.
12. P. D. BAYER and R. E. COOPER, *J. Mater. Sci.* **2** (1967) 233.

13. R. MARCHAND, Y. LAURENT, J. LANG and M. T. L. BIHAN, *Acta Cryst.* **B25** (1969) 2157.
14. K. INOMATA and Z. INOUE, *Yogyo-Kyokai-Shi* **81** (1973) 441.
15. W. D. FORGENG and B. F. DECKER, *Trans. Met. Soc. AIME* **212** (1958) 343.
16. C. R. BROOKES, J. B. O'NEILL and B. A. W. REDFERN, *Proc. Roy. Soc. Lond.* **A322** (1971) 73.
17. R. H. HANNINK, D. L. KOHLSTEDT and J. MURRY, *ibid.* **A326** (1972) 409.
18. G. MORGAN and M. H. LEWIS, *J. Mater. Sci.* **9** (1974) 349.
19. D. J. ROWCLIFFE and G. E. HOLLOX, *ibid.* **6** (1971) 1261.
20. O. O. ADEWOYE and T. F. PAGE, *ibid.* **11** (1976) 981.
21. Y. KUMASHIRO, A. ITOH, T. KINOSHITA and M. SOBAJIMA, *ibid.* **12** (1977) 595.
22. K. NAKANO and H. MATSUBARA, *J. Less-Common Metals* **47** (1976) 259.
23. D. J. ROWCLIFFE and G. E. HOLLOX, *J. Mater. Sci.* **6** (1971) 1270.
24. K. NIIHARA and T. HIRAI, *ibid.* **12** (1977) 1233.
25. K. KIJIMA, Report of National Institute of Inorganic Materials in Japan, no. 13 (1977) 1.
26. K. KIJIMA, K. KATO, Z. INOUE and H. TANAKA, *J. Mater. Sci.* **10** (1975) 362.
27. K. NIIHARA, *J. Less-common Metals* (to be published).
28. F. W. VAHLDIEK and S. A. MERSOL, *J. Less-Common Metals* **55** (1977) 265.
29. H. PALMOUR III, W. W. KRIEGEL and J. J. DUPLESSIS, "Mechanical Properties of Engineering Ceramics", edited by W. W. Kriegel and H. Palmour III (Interscience, New York, 1961) p. 313.
30. K. NIIHARA and T. HIRAI, *J. Mater. Sci.* **13** (1978) 2276.
31. *Idem,* unpublished data.
32. R. D. KOESTER and D. P. MOAK, *J. Amer. Ceram. Soc.* **50** (1967) 290.
33. L. BSENKO and T. LUNDSTROM, *J. Less-Common Metals* **34** (1974) 273.
34. J. H. WESTBROOK, Rev. *Hautès Temp. Rèfract.* **3** (1966) 47.
35. T. HIRAI and K. NIIHARA, *J. Mater. Sci.* (to be published).
36. A. G. EVANS and J. V. SHARP, *ibid.* **6** (1971) 1292.
37. R. KOSSOWSKY, *ibid.* 8 (1973) 1603.

Received 3 November and accepted 27 November 1978.